

Segmental and chain dynamics in a diblock copolymer melt near the microphase separation transition

G. Fytas* and A. Rizos

Foundation for Research and Technology – Hellas, PO Box 1527, 71110 Heraklion, Crete, Greece

and I. Alig and F. Kremer

Max-Planck Institut für Polymerforschung, PO Box 3148, 6500 Mainz, Germany

and J. Roovers

National Research Council of Canada, Ottawa, Ontario, K1A 0R6, Canada

(Received 22 April 1992; revised 15 September 1992)

The dynamics of segmental and chain orientation in poly(styrene-*b*-isoprene) (P(S-*b*-I)) block copolymer with PI fraction $f_{PI}=0.61$, degree of polymerization $N=70$ and $\chi N \approx 9$ at 25°C (χ is the interaction parameter) were investigated by depolarized Rayleigh scattering (DRS) and dielectric spectroscopy (d.s.) over a broad temperature range (240–370 K) in the disordered phase. Two distinct primary relaxation processes with vastly different timescales were associated with segmental orientation within PS- and PI-rich regions selectively probed by DRS and d.s. techniques. The width of the distribution relaxation function for the slow segmental process was found to increase with decreasing temperature, whereas the freezing of the slow segmental fluctuations was observed for the first time within the time window of photon correlation spectroscopy. Compared with an equivalent PI homopolymer chain, the first normal mode describing the end-to-end fluctuation of the copolymer chain displayed slower time τ_1 but similar amplitude $\delta\epsilon_N/f_{PI}$. The new experimental results were discussed in terms of the fluctuation picture of block copolymers in the disordered melt, the chain conformation and the friction coefficient ratio of the foreign blocks.

(Keywords: dynamics; block copolymer; microphase separation; polystyrene; polyisoprene; relaxation; light scattering; dielectric spectroscopy)

INTRODUCTION

Unlike polymer blends, diblock copolymers A–B are single-component systems, and hence cannot separate macroscopically but *can* exhibit microphase segregation¹. Their phase diagram is dominated by the block composition $f=N_A/N$ and the product χN of the segment–segment interaction parameter χ and the total degree of polymerization $N=N_A+N_B$. In the mean-field theory², above the microphase separation transition (m.s.t.), i.e. $\chi N < (\chi N)_s$, the amplitude of the composition fluctuations $\langle \psi_q^2 \rangle$ is predicted to be very small; ψ_q is the Fourier transform of $\psi(r)=\rho_A(r)/\rho-f$ where $\rho_A(r)$ is the local density of A segments and ρ the overall (A plus B) segment density. However, inclusion of fluctuation effects³ in the mean-field theory led to significant $\langle \psi_q^2 \rangle$ with characteristic length $\xi \sim RN^{1/6}$ (R = radius of gyration) in the disordered phase.

In the mean-field theory^{4–6}, the dynamics of $\psi(q,t)$ fluctuations are determined by the thermal decay time τ , which in the small- q limit is independent of q and for Gaussian chains becomes proportional to N^2 . Hence, τ should be comparable to the timescale τ_1 of the

end-to-end fluctuation of the copolymer chain, i.e. the long-wavelength first normal mode. Conversely, the faster segmental dynamics with correlation length ξ_g (≈ 10 Å) characteristic of the glass transition^{7,8} are independent of N and determined by the local friction coefficient ζ in the slowly fluctuating chain environment. In this fluctuation picture³, the chemically different segments of A and B blocks move in a stationary environment rich in either A or B, and hence could exhibit two different primary relaxation times, since the friction coefficients ζ_A and ζ_B of the pure homopolymers are usually different. It therefore becomes apparent that a study of both segmental and chain dynamics of diblock copolymers at various proximities from the m.s.t. will help to document experimentally these theoretical predictions.

Concerning the conformation of a diblock copolymer in the melt, recent Monte Carlo simulations⁹ and analytical calculations¹⁰ suggest a cigar-like form resulting from the partially separated A and B blocks. This form persists even for athermal ($\chi=0$) copolymers, thus rationalizing the presence of two distinct primary processes in polyisoprene-*b*-poly(1,2-butadiene) (PI–PVE)¹¹ with $\chi \approx 10^{-4}$. A direct measure of the copolymer conformation would be the mean-square end-to-end distance, which affects the longest relaxation of the

* To whom correspondence should be addressed

Table 1 Molecular characteristics

Sample	Isoprene (wt%)	M_n (PS)	M_n (total)	T_g (K)	$(\chi N)_{25^\circ\text{C}}^a$
P(S- <i>b</i> -I)	50.4	2830	5700	248 ± 25	8.9

^aRef. 17

chain¹². The latter can best be studied by dielectric spectroscopy (d.s.) provided there is a dipole moment component along the chain contour. The most well known, out of few such polymers, is *cis*-polyisoprene (PI).

In the present paper, we report on segmental and chain motions in poly(styrene-*b*-isoprene) (P(S-*b*-I)) copolymer for the first time in the disordered phase. This system was chosen on account of its known interaction parameter χ , the relatively large value of the optical anisotropy $\langle\gamma^2\rangle$ per monomer of PS, the dielectric activity of the normal mode of the PI subchain and the large disparity between the values of ζ_A and ζ_B . Thus, depolarized light scattering¹³ and d.s.¹⁴ can be employed to measure both segmental and chain orientation. The used P(S-*b*-I) sample designed to be in the disordered phase has $f_{PI}=0.61$, $N=70$ and hence $\chi N=8.9$ at 25°C. The dielectric normal mode of the subchain PI anchored on the microdomain boundary of microphase-separated P(S-*b*-I) diblock copolymers has recently been studied¹⁵. The time τ_1 is exclusively determined by the PI microdomains. A second dielectric study deals with homogeneous PI-1,4-polybutadiene (PI-PBD) in which the normal mode of the PI block depends on the molecular weight of the whole chain¹². In the present thermally homogeneous P(S-*b*-I) sample with vastly different ζ_{PS} and ζ_{PI} , a significant retardation of the end-to-end fluctuations of the chain was predicted and found, which, based on the dielectric strength, displays an extended conformation in the melt. Moreover, the presence of two well separated primary relaxation processes, intermediate to the dynamics of the constituent homopolymers, reveals significant composition fluctuations in the P(S-*b*-I) sample. The freezing-in first of the PS segmental fluctuations as the temperature decreases affects the normal-mode dynamics of P(S-*b*-I).

EXPERIMENTAL

Sample

The diblock copolymer poly(styrene-*b*-*cis*-1,4-isoprene) has been prepared by anionic polymerization. The sample characteristics¹⁶ are summarized in Table 1.

Photon correlation spectroscopy

The time correlation function $G(t)$ of the depolarized scattering intensity for the diblock copolymer was measured at a scattering angle $\theta=90^\circ$ at different temperatures between -27 and 50°C . The light source was an Ar⁺ laser (Spectra Physics 2020) operating at 488 nm with a power of 250 mW. The incident beam was polarized vertically (V) with respect to the scattering plane and the light scattered from the sample was collected through a Glan-Thompson analyser with an extinction coefficient better than 10^{-7} . The scattered light was polarized parallel (H) to the incident laser beam. The VH intensity autocorrelation functions were measured over eight decades in time with an ALV5000 multibit correlator with 280 logarithmically spaced channels. In

a homodyne experiment the desired normalized field $g(t)$ is related to $G(t)$ by:

$$G(q, t) = A[1 + f^*|\alpha g(q, t)|^2] \quad (1)$$

where A is the baseline measured at long log times, f^* is the instrumental factor calculated by means of a standard PS/CCl₄ dilute solution and α is the fraction of the total depolarized scattering intensity arising from fluctuations in the optical anisotropy with correlation times longer than 10^{-6} s.

Dielectric spectroscopy

The dielectric measurements covered the frequency range from 10^{-2} to 10^6 Hz, using a Solartron-Schlumberger frequency response analyser FRA-1254. The sample was kept between two gold-plated stainless-steel electrodes (diameter 20 mm) with a spacing of 50 ± 1 μm maintained by two fused silica fibres. Using a temperature-controlled nitrogen gas jet and a custom-made cell, temperature adjustment over a broad range was achieved.

RESULTS

The time correlation functions of the depolarized light scattering intensity shown in Figure 1 display a broad and temperature-dependent shape. The fit of the well known Kohlrausch-Williams-Watts (KWW) function:

$$C(t) = \exp[-(t/\tau)^\beta] \quad (2)$$

yields for the shape parameter β the values 0.25 and 0.14 respectively at 30 and 7°C. For comparison, $\beta=0.35$ and 0.44 for the bulk homopolymers PS and PI respectively. The fraction $\alpha(=bf^{*1/2})$ of the depolarized Rayleigh intensity with correlation times longer than about 10^{-6} s is lower than one and hence indicates the presence of two relaxation processes with different timescales. A rough estimate of α , based on the contribution of PS segmental orientation, can be obtained from the PS composition in the copolymer and the values of $\langle\gamma^2\rangle_{PS}=38 \text{ \AA}^6$ and $\langle\gamma^2\rangle_{PI}=11 \text{ \AA}^6$ for the optical anisotropies per monomer of the two homopolymers in solution¹⁸. The computed value of $\alpha(=0.69)$ compares favourably with the fast time intercept of $C(t)$, which, therefore, reflects the segmental dynamics of PS block. The fit of the KWW function reveals, however, systematic deviations in the residuals plot.

An alternative fitting procedure, without an *a priori* assumption of the form of the distribution relaxation function but assuming a superposition of exponentials,

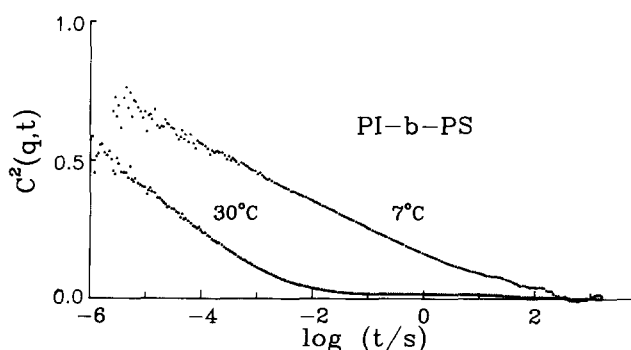


Figure 1 Net depolarized intensity correlation functions $(C(q, t))^2$ of P(S-*b*-I) block copolymer at two temperatures, above T_g

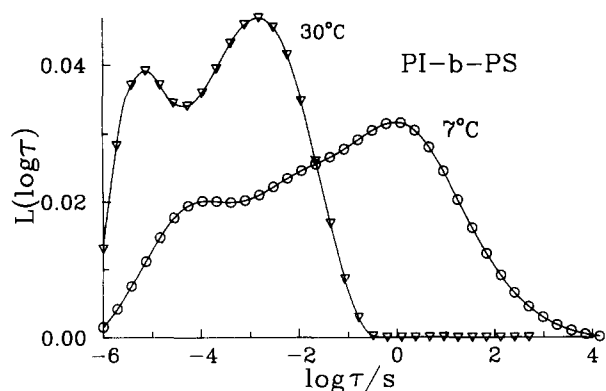


Figure 2 Distribution of segmental orientation times within PS-rich region obtained from the inversion of $C(t)$ in *Figure 1*

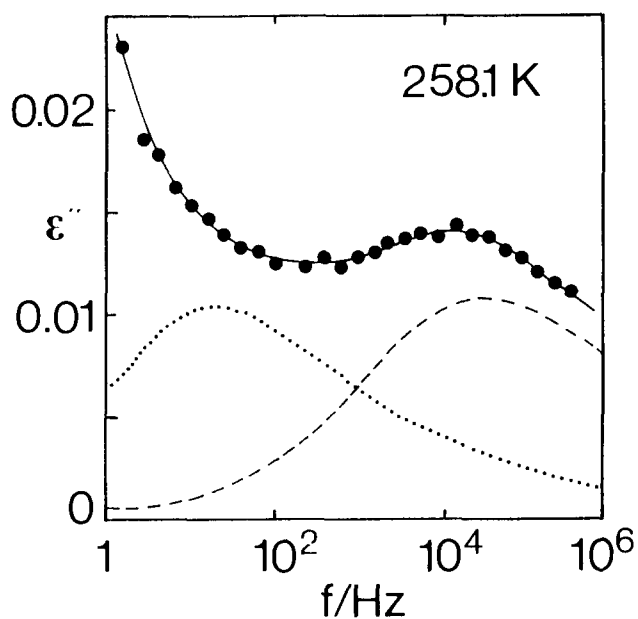


Figure 3 Dielectric loss ϵ'' for segmental orientation within PI-rich region at -15°C . Full curve denotes the fit of equation (4) considering the contribution of the slow chain motion (dotted curve) and d.c. contribution. The broken curve is for the contribution of the segmental orientation alone

is the inverse Laplace transformation¹⁹ (ILT) of the experimental $C(t)$:

$$C(t) = \int_{-\infty}^{\infty} d \ln \tau L(\ln \tau) e^{-t/\tau} \quad (3)$$

The distribution of orientational times $L(\ln \tau)$ is shown in *Figure 2*. The amplitude $\alpha = \int_{-\infty}^{\infty} d \ln \tau L(\ln \tau)$ amounts to 0.7 at 7°C . We conclude, therefore, that there exists a further fast fluctuating anisotropic intensity resulting in an asymmetric broadening of $L(\ln \tau)$ at short times. An average $\langle \log \tau \rangle$ from the distribution and a characteristic time $\log \tau_{\max}$ for which the distribution assumes its maximum value can be obtained from *Figure 2*. If the origin of the broadening of $L(\ln \tau)$ beyond that of the pure PS is the presence of composition fluctuations, then $\log \tau_{\max}$ emphasizes segmental dynamics in a PS-rich environment. The still missing faster segmental orientation of PI is better resolved in the dielectric loss $\epsilon''(\omega)$ data, owing to the much higher dipole moment of PI monomer compared to that of PS. In fact the fast

peak of $L(\log \tau)$ in *Figure 2* might be attributed to segmental dynamics within the PI-rich region.

Figure 3 depicts the dispersion in $\epsilon''(\omega)$ for PS-PI at 15°C . This low- T broad peak is associated with the segmental dynamics of PI block being, indeed, faster than PS. As we will see below (*Figure 4*), the normal mode of the copolymer chain, dielectrically active through the PI block, is slower and, hence, appears at higher T . Over the T range 233 to 268 K a segmental relaxation time $\tau = 1/(2\pi f_{\max})$ can be determined as the inverse of the loss maximum frequency f_{\max} . To estimate, however, the breadth of the underlying distribution the Havriliak-Negami (HN) function was used to fit²⁰ these broad and asymmetric loss curves:

$$\epsilon^*(\omega) - \epsilon_\infty = \Delta\epsilon / [(1 + i\omega\tau_{\text{HN}})^\alpha]^\gamma \quad (4)$$

$\Delta\epsilon$ denotes the relaxation strength, ϵ_∞ is the limiting high-frequency ϵ' , and τ_{HN} , α and γ are the HN relaxation parameters. The full curve in *Figure 3* denotes HN fits to the experimental $\epsilon''(\omega)$ considering the normal mode and the electrical conductivity contribution at low frequencies. It is worth mentioning that the $\Delta\epsilon$ for segmental relaxations is in agreement with the corresponding value of bulk PI weighted by the PI composition in the copolymer. This constitutes an additional support to the assignment of the peaks in *Figure 3* to the primary relaxation of a PI block in a PI-rich environment.

There is a second dielectric dispersion in PS-PI copolymer at higher T , as shown in *Figure 4*. These $\epsilon''(\omega)$ peaks are narrower than those in *Figure 3* and are assigned to the normal-mode process of the chain. The HN fit can be performed more easily at high T , for which the overlap with the segmental relaxation (*Figure 3*) can be ignored. Unlike the situation for the segmental mode of PI, the normal-mode peak in P(S-*b*-I) is characterized by $\Delta\epsilon$ as large as in bulk PI. In addition, the loss curves of *Figure 4* are broader than that of PI homopolymer. These pertinent findings will be discussed in the next section. The results of the HN fits to the segmental

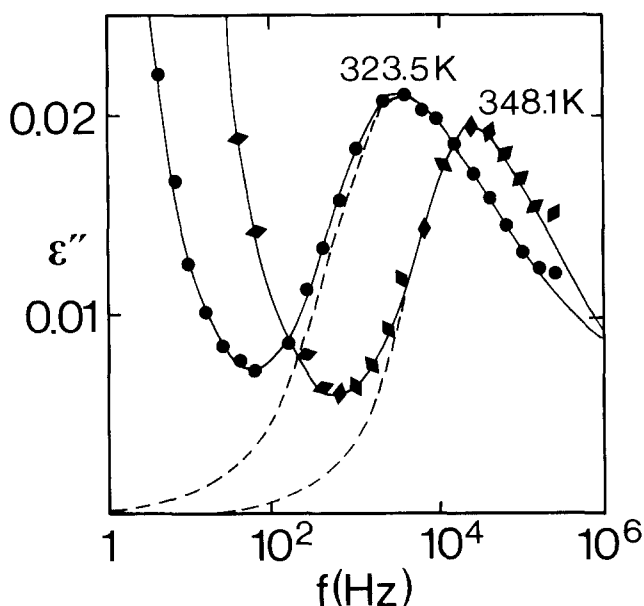


Figure 4 Dielectric loss ϵ'' for end-to-end chain orientation at 50.4 and 75°C . The broken curves show the contribution of the normal-mode motion alone

Table 2 Distribution parameters for segmental and normal-mode process

Segmental			Normal mode							
$T(^{\circ}\text{C})$	β		$T(^{\circ}\text{C})$	α	γ	β	$T(^{\circ}\text{C})$	α	γ	β
45	0.31	-15	0.49	0.38	0.26	75	0.86	0.33	0.37	
38	0.29	-20	0.57	0.38	0.29	65	0.82	0.33	0.35	
30	0.25	-25	0.61	0.38	0.31	55	0.80	0.31	0.32	
25	0.23	-30	0.48	0.38	0.25	45	0.70	0.37	0.31	
14	0.20					35	0.60	0.44	0.34	
7	0.14					25	0.56	0.44	0.32	

and normal modes of the P(S-*b*-I) sample and the corresponding KWW β are listed in Table 2.

DISCUSSION

The depolarized light scattering and dielectric spectroscopic results provide significant information on the local structure of symmetric diblock copolymer melts in the disordered phase. In this section, we rationalize the pertinent experimental findings in terms of the fluctuation picture and address questions concerning the theoretical description of diblock dynamics.

Segmental relaxation processes

The peak location in the $L(\log \tau)$ (Figure 2) and $\epsilon''(\omega)$ (Figure 3) plots indicates the presence of two relaxation processes with vastly different timescales. The dielectric response is due to PI segment orientation associated with the glass-rubber relaxation within the PI-rich region. In fact, the thermodynamic single glass transition extends over a broad T range from -50 to 0°C . On the other hand, it is not obvious what dominates the correlation function $C_{\text{VH}}(t)$ (Figure 1). In principle, both local segmental orientation fluctuations and overall molecular orientation can modulate the depolarized Rayleigh scattering from bulk polymers consisting of optical anisotropic segments²¹:

$$C_{\text{VH}}(t) = \left\langle \sum_{ij} \alpha_{yz}(j, t) \alpha_{yz}(i, 0) \exp\{iq[r_j(t) - r_i(0)]\} \right\rangle \quad (5)$$

where $\alpha_{yz}(j, t)$ is the yz component of the laboratory-fixed polarizability tensor of the j th segment at $r_j(t)$ and $\langle \rangle$ denotes a statistical average. (In the commonly used anisotropic scattering geometry the incident beam propagates in the xy plane with polarization parallel to the z axis and the scattered light is observed in the y direction.) For light scattering q values, the phase term in (5) is not very different from unity and hence $C_{\text{VH}}(t)$ is q -independent, as verified experimentally, and dominated by fluctuations in α_{yz} . In particular for diblock copolymers, which are predicted^{9,10} to display an elongated 'cigar-like' gross shape, molecular orientation could affect²² $C_{\text{VH}}(t)$. However, the fair account for the amplitude of $C_{\text{VH}}(t)$ by the optical anisotropy of PS block alone supports the assignment of $C_{\text{VH}}(t)$ to segmental orientational dynamics of PS. In addition, the much broader distribution of this process as compared to the chain normal mode (Table 2) corroborates this assignment. In this context, a molecular-weight-dependent study will be very helpful.

Figure 5 presents an Arrhenius plot of the two segmental orientation times τ_r and τ_s obtained from the

peak location of $\epsilon''(\omega)$ and $L(\log \tau)$ respectively. For the bulk homopolymers PI ($T_g = 207$ K) and PS ($T_g = 340$ K), the primary relaxation times obtained from DR²⁰ and p.c.s. experiments are also shown in Figure 5 for comparison. The segmental dynamics of PI and PS blocks are apart by eight decades in time at about 5°C , but lie between the primary times of the two homopolymers. According to this finding, the P(S-*b*-I) sample is not fully microphase separated. Microphase-segregated diblock copolymers exhibit two distinct primary processes, which coincide with the corresponding dynamics in the homopolymers^{23,24}. The homogeneity of the sample is also suggested by the value of χN . Using the reported¹⁷ T dependence $\chi = -0.094 + 66/T$ also verified in binary blends of low-molecular-weight PS and PI, the factor χN varies from 10.5 to 5.6 over the T range 0 to 100°C .

In the Arrhenius plot of Figure 5, the primary relaxation curves for PS-rich and PI-rich environments in the symmetric diblock copolymer are significantly shifted from the corresponding lines for the pure phases. Assuming a linear dependence between $1/T_g$ and copolymer weight fraction, a rough estimate of the PIP composition within the PS-rich region is 0.37 and within the PI-rich environment 0.78. Note that the weight-average PI fraction in the copolymer is 0.5. These significant deviations from the mean value support the fluctuation picture³ of block copolymers in the disordered phase. A clear resolution of two primary processes was recently found in rheologically homogeneous nearly symmetric polystyrene-poly(methylphenylsiloxane) (PS-PMPS) diblock copolymer²⁴ with $\chi N \approx 3$ by combined DRS-p.c.s. and d.s. data. At the overlapping $T = 35^{\circ}\text{C}$ the ratio $\tau(\text{PS})/\tau(\text{PMPS})$ in the copolymer amounts to 10^7 . In both cases, the distribution parameter β for segmental orientation within the PS-rich region decreases significantly with decreasing T (Table 2). However, it appears that in a PI-rich environment the distribution is narrower (higher β) than in a PS-rich region. Whereas there is no quantitative account for the value of β in bulk homopolymers so far, this excess broadening of the distribution is probably related to the amplitude of the composition fluctuations $\langle \psi_q^2 \rangle$ with correlation length ξ .

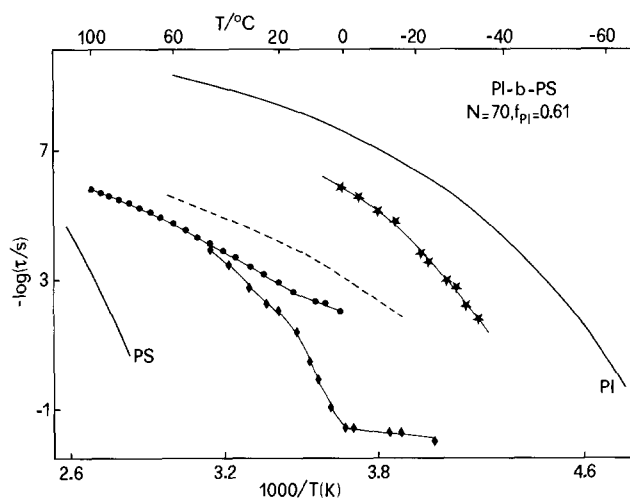


Figure 5 Relaxation rates for segmental motion within PI- and PS-rich regions (* and ● respectively) and normal-mode motion (◆) of P(S-*b*-I) copolymer chain. Full curves are for the segmental relaxation rates in bulk PI and PS homopolymers whereas the broken curve denotes the relaxation rate for the first normal mode of an equivalent PI chain (see text)

The different β values of Table 2, however, imply that $\langle \psi_q^2 \rangle$ alone cannot account for the width of the two distributions.

In the coupling scheme of relaxation, the broad single dynamic mechanical loss in entropically mixed ($\chi=0$) PI/PVE blends²⁵ has been represented by assuming a Gaussian distribution of β values around the mean values β_i of the pure homopolymers. The breadth $\langle \delta\beta^2 \rangle$ of the Gaussian distribution was considered as a measure of the concentration fluctuations. Because of the considerable number of adjustable parameters, there was no explicit relation for the amplitude of the concentration fluctuations in this well miscible blend. Alternatively, for the athermal PI-PVE diblock¹¹ both DRS-p.c.s. and d.s. techniques have shown bimodal primary relaxation. However, compared to the present results the peak separation was much smaller (~ 2 decades in time) and the shape of $C_{\text{vH}}(t)$ was virtually T -independent. The dual feature of the primary relaxation in the isotropic ($\chi=0$) PI-PVE ($N=107$) melt is a hint of the role of a second length $\xi_g (\sim V_g^{1/3})$ associated with the main glass transition, which is generally accepted to involve few monomer units^{7,8}, i.e. $\xi_g \approx 10 \text{ \AA}$. If a diblock PI-PVE chain assumes a 'cigar-like' form^{9,10,22} with blocks separated along the direction of the end-to-end vector, then the situation $\xi_g < R$ can rationalize the experimental findings provided the two homopolymers have sufficiently different mobilities. The closeness between the T_g values of PI and PBD might explain the single segmental ϵ'' peak in PI-PBD copolymer melt¹².

In view of these concepts, the larger amplitude $\langle \psi_q^2 \rangle$ in the less homogeneous ($\chi N \approx 9$ at 25°C) PI-PS copolymer melt, along with the large difference $T_g(\text{PS}) - T_g(\text{PI}) \approx 130 \text{ K}$ of its constituent homopolymers, should lead to larger separation of the primary relaxation times (Figure 5) compared to the PI-PVE system. With decreasing T both ξ_g and τ_s/τ_f increase. The increase of the former facilitates the probing of more heterogeneous environments and hence results in a broader (lower β) distribution as observed experimentally within the PS-rich region. Alternatively, in the PI-rich region the effect due to the increase of ξ_g is probably compensated by the frozen-in segmental dynamics of PS and β is therefore insensitive to T variations. For the fluctuations $\psi(q, t)$ in disordered block copolymers it is generally assumed^{5,6} that their dynamics are slower than the segmental fluctuations as mentioned in the introduction. The freezing of the PS segmental dynamics is an interesting effect observed for the first time by p.c.s. This behaviour in bulk homopolymers has been anticipated for a long time, as a consequence of the kinetic nature of the glass transition. The lack of experimental documentation in bulk PS and other bulk polymers²⁶ is due to the very slow times not accessible by p.c.s. The present observation in P(S-*b*-I) diblock copolymer is, in fact, a manifestation of composition fluctuations, which increase the fractional free volume f_g (at T_g) within the PS-rich microregions compared to the PS homopolymer. Therefore, the freezing of the slow primary relaxation occurs at rates faster than the low time limit of p.c.s.

Chain normal-mode relaxation

For the present low-molecular-weight P(S-*b*-I) the timescales characteristic of segmental motion of PI and normal-mode relaxation of the copolymer chain ($N=70$) are separated more than we would anticipate for a PI

chain of the same length in the bulk state. Figure 6 shows the T variation of $\epsilon''(T)$ for P(S-*b*-I) at three frequencies. The low- T and high- T peaks are assigned to segmental orientation within the PI-rich region and chain normal-mode motion respectively. At 10^3 Hz the two loss peaks occur at temperatures almost 70 K apart; in bulk PI²⁰ the corresponding difference is about 30 K.

We have computed the relaxation time τ_1 for the first normal mode of the P(S-*b*-I) copolymer chain from the segmental relaxation time of bulk PI ($M_w=5100$, figure 4a of ref. 19) assuming N^2 dependence. However, these relaxation times of chain orientation are referred to the local friction of the bulk PI (full curve in Figure 5). Therefore, a T shift of 21 K, necessary to superimpose the segmental dynamics of PI in bulk and in copolymer, is required to compute τ_1 for P(S-*b*-I) (broken curve in Figure 5). Parenthetically, the constant shift factor for the segmental dynamics in bulk PI and P(S-*b*-I) over the T range 233 to 273 K suggests that the PI segments are moving in domains rich in PI.

The computed values of τ_1 are about 10 times faster than the experimental values (full circles in Figure 5). This slowing down of the normal-mode motion of the P(S-*b*-I) chain, observed for the first time in diblock copolymers in the disordered phase, can be due to the difference in the monomeric friction coefficients of foreign blocks²⁷ and/or to thermodynamic slowing down^{5,6} of composition fluctuations with $q^* \sim 2/R$. According to the former prediction²⁷ the normal-mode spectrum and τ_1 of homogeneous block copolymers (for free-draining conditions) depends sensitively on block composition and friction coefficient ratio. Numerical evaluation of the discrete Rouse spectrum of a diblock A-B with composition $f_B=0.68$ for the mobile component assuming the same spring constants for A and B chains has revealed significant retardation of $\tau_1(\text{B})$ for the homopolymer; for $\zeta_A/\zeta_B=185$, $\tau_1(\text{AB})/\tau_1(\text{B}) \approx 20$ which increases to 10^3 when the friction ratio rises to 10^4 . Whereas the former numerical result offers a qualitative account for the pertinent experimental finding, a quantitative description is precluded mainly because the values of ζ_A/ζ_B and chain dimensions to be assigned to the blocks are not known. Alternatively, the thermodynamic slowing-down effect^{5,6} near q^* estimated on the basis of the mean-field theory

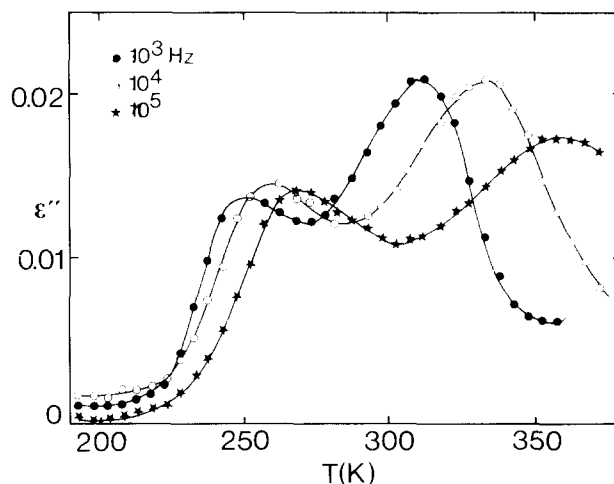


Figure 6 Variation of the dielectric loss ϵ'' of P(S-*b*-I) block copolymer with temperature at three frequencies. The low- T and high- T peaks are assigned to segmental motion within PI-rich region and normal-mode motion of the chain respectively

is $(\chi N)_s/[(\chi N)_s - (\chi N)] \approx 3$ for the present sample at 25°C. For experimental verification of this effect, normal-mode measurements on P(S-*b*-I) of constant composition but different N are in progress.

The segmental relaxation times, being a measure of the local friction coefficient of the copolymer component, are referred to the regions rich in either block, i.e. ζ_{PS}/ζ_{PI} ($\sim 10^3$ at 50°C, see *Figure 5*) is severely overestimated. Conversely, the end-to-end fluctuations of the P(S-*b*-I) chain having comparable dynamics with the fluctuating composition pattern are dominated by effective friction coefficients averaged over the different regions. It therefore appears plausible that the effective ratio $(\zeta_{PS}/\zeta_{PI})^*$ for chain motion should assume a much smaller value than ζ_{PS}/ζ_{PI} . Moreover, like the situation in a mixed glass, the overall friction ζ^* for chain motion should lie between ζ_{PS} ($\sim \tau_s$) and ζ_{PI} ($\sim \tau_f$) in the Arrhenius plot of *Figure 5*. In fact, a crude estimate of the T dependence of ζ^* is obtained by shifting the curve $\tau_f(T)$ by ΔT necessary to superimpose the broken curve with the experimental $\tau_1(T)$.

An additional cause for slowing down of the normal-mode motion of P(S-*b*-I) chain can be the 'tethering' effect for the PI subchains. For microphase-separated P(S-*b*-I) samples¹⁵ the long-wavelength motion of the PI subchain tethered on the frozen PS wall should become slower by a factor 4 compared to the case with both ends free. In the present disordered P(S-*b*-I) sample, however, the PS subchains become glasses below about 273 K. In this T range, the tethering effect can be relevant, accounting partially for the disparity between the experimental and calculated τ_1 values in *Figure 5*.

An intriguing feature in *Figure 5* is the closeness between chain normal mode and PS segmental dynamics at high T and the change in the T dependence of τ_1 when τ_s becomes longer than τ_1 . At first glance, this observation appears less meaningful since the segmental motion is generally accepted to be the precursor of the chain normal-mode dynamics. Here, we recall that τ_s is obtained from the long-time peak of $L(\log \tau)$ (*Figure 2*), which arises from slow segmental fluctuations within the PS-rich region. In view of the preceding discussion, this result corroborates the notion that the effective ζ_{PS}^* for chain motion is less than $\zeta_{PS} \sim \tau_s$. Moreover, τ_1 for P(S-*b*-I) is faster than the relaxation time for long-wavelength motion of an equivalent PS homopolymer chain due to the smaller friction of the PI block. However, with further decrease of T below about 30°C, τ_s increases faster than τ_1 and hence no longer can determine the value of τ_1 . In fact, the latter appears to display weaker T dependence as if the PS block dynamics were switched off. Nevertheless, a quantitative description of the values and the T variation of the different timescales of *Figure 5* is still missing.

Chain conformation

The dielectric relaxation strength $\Delta\epsilon$ associated with the PI segmental motion and PI-PS chain motion can be obtained from the fit of equation (3) to the $\epsilon''(\omega)$ data. Over the T range 240 to 260 K, $\Delta\epsilon_{seg}$ for the primary relaxation of PI in P(S-*b*-I) copolymer amounts to 0.06 ± 0.02 . This value is less than $\Delta\epsilon_{seg} (\approx 0.1)$ for PI homopolymer²⁰ over the same T range and scales roughly with the PI composition. Conversely, $\Delta\epsilon_N$ for normal mode of P(S-*b*-I) chain varies from 0.07 at 373 K to 0.11 at 281 K compared to the corresponding values

0.08 and 0.10 of $\Delta\epsilon_N(\text{PI})$ in bulk PI; clearly, there is an enhancement of the dielectric dispersion associated with the chain normal mode of the PI-PS chain. The strength $\Delta\epsilon_N$ is given by¹¹:

$$\Delta\epsilon_N = \frac{4\pi N_A \mu^2 \langle r_{nm}^2 \rangle f_{PI}}{3k_B T M_{PI}} \quad (6)$$

where N_A is Avogadro's constant, μ is the dipole moment per unit contour length, $\langle r_{nm}^2 \rangle$ the mean-square distance of the PI block in the copolymer with weight fraction f_{PI} and M_{PI} is the molecular weight of the PI subchain. Comparison between the values of $\Delta\epsilon_N(\text{PI-PS})/f(\text{PI})$ and $\Delta\epsilon_N(\text{PI})$ indicates that either the PI block is significantly expanded assuming a stretched-coil conformation well into the disordered state of P(S-*b*-I) copolymer and/or there exists a significant amount of positive segmental pair correlations (i.e. increase of μ). Based on SANS from symmetric copolymer melts a change from Gaussian to stretched-coil conformation was recently reported^{28,29} to occur well below the order-disorder transition suggested also by Monte Carlo simulations⁹. On the other hand, from dielectric measurements on PI-PBD copolymer melts¹² a Gaussian conformation for PI block chain was concluded. However, this interesting result must be further verified on chains of different length and hence different proximity to m.s.t.

CONCLUDING REMARKS

The bimodal character of the segmental relaxation along with the T dependence of the corresponding distributions $L(\log \tau)$ can be rationalized by the presence of a significant amount of composition fluctuation $\langle \psi_q^2 \rangle$ in the disordered P(S-*b*-I) copolymer melt. However, no quantitative relationship between the observed broadening of $L(\log \tau)$ and $\langle \psi_q^2 \rangle$ and correlation volume ξ_g^3 is known as yet. The normal-mode motion of the copolymer P(S-*b*-I) chain in the homogeneous melt is subject to considerable retardation due to the less mobile PS block and becomes faster than the segmental dynamics within a PS-rich environment. This finding constitutes a further support of large $\langle \psi_q^2 \rangle$ in the disordered P(S-*b*-I) copolymer ($\chi N = 9$ at 25°C). A theoretical calculation of the first normal-mode time τ_1 in copolymers with $\chi N \neq 0$ is still missing. Unfavourable segment-segment interactions can be responsible for a stretched-coil conformation of PI block implied by the dielectric loss associated with τ_1 .

ACKNOWLEDGEMENTS

The financial support of the FORTH and MPI-P is gratefully acknowledged. G.F. thanks Dr S. Anastasiadis for stimulating discussions.

REFERENCES

- 1 Bates, F. S. and Fredrickson, G. H. *Annu. Rev. Phys. Chem.* 1990, **41**, 525 and references therein
- 2 Leibler, L. *Macromolecules* 1980, **13**, 1602
- 3 Fredrickson, G. H. and Helfand, E. *J. Chem. Phys.* 1987, **87**, 697
- 4 Akcasu, A. Z., Benmouna, M. and Benoit, H. *Polymer* 1986, **27**, 1935
- 5 Fredrickson, G. H. *J. Chem. Phys.* 1986, **85**, 5306
- 6 Onuki, A. *J. Chem. Phys.* 1987, **87**, 3692
- 7 Fischer, E. W., Donth, E. and Steffer, W. *Phys. Rev. Lett.* 1992, **68**, 2344

- 8 Matzuoka, S. and Quan, X. *Macromolecules* 1991, **24**, 2770
- 9 Fried, H. and Binder, K. *J. Chem. Phys.* 1991, **94**, 8349
- 10 Barrat, J. L. and Fredrickson, G. H. *J. Chem. Phys.* 1991, **95**, 1281
- 11 Kanetakis, J., Fytas, G., Kremer, F. and Pakula, T. *Macromolecules* 1992, **25**, 3484
- 12 Adachi, K., Nishi, I., Doi, H. and Kotaka, T. *Macromolecules* 1991, **24**, 5843
- 13 Rizos, A., Fytas, G. and Roovers, J. E. L. *J. Chem. Phys.* 1992, **97**, 6925
- 14 Alig, I., Kremer, F., Fytas, G. and Roovers, J. E. L. *Macromolecules* 1992, **25**, 5277
- 15 Yao, M. L., Watanabe, H., Adachi, K. and Kotaka, T. *Macromolecules* 1991, **24**, 2955
- 16 Toporowski, P. M. and Roovers, J. E. L. *J. Polym. Sci., Polym. Chem. Edn.* 1976, **14**, 2233
- 17 Mori, K., Haseguwa, H. and Hashimoto, T. *Polym. J.* 1985, **17**, 799
- 18 Saiz, E., Floudas, G. and Fytas, G. *Macromolecules* 1991, **24**, 5796
- 19 Provencher, S. W. *Comput. Phys. Commun.* 1982, **27**, 213
- 20 Boese, D. and Kremer, F. *Macromolecules* 1990, **23**, 829
- 21 Zero, K. and Pecora, R. in 'Dynamic Light Scattering' (Ed. R. Pecora), Plenum Press, New York, 1985
- 22 Pakula, T. *J. Chem. Phys.* 1991, **95**, 4685
- 23 Quan, X., Johnson, G. E., Anderson, E. W. and Bates, F. S. *Macromolecules* 1989, **22**, 2451
- 24 Gerharz, B., Fischer, E. W. and Fytas, G. *Polym. Commun.* 1991, **32**, 469; Gerharz, B., Vogt, S., Fytas, G. and Fisher, E. W. *Colloid Polym. Sci.* in press
- 25 Roland, C. M. and Ngai, K. L. *Macromolecules* 1991, **24**, 4261
- 26 Meier, G. and Fytas, G. in 'Optical Techniques to Characterize Polymer Systems' (Ed. E. Bassler), Elsevier Scientific, Amsterdam, 1989, p. 535
- 27 Hansen, D. and Shen, M. *Macromolecules* 1975, **8**, 343
- 28 Almdal, K., Rosedale, J. H., Bates, F. S., Wignall, G. D. and Fredrickson, G. H. *Phys. Rev. Lett.* 1990, **65**, 1112
- 29 Holzen, B., Lehmann, A. and Stühn, B. *Polymer* 1991, **32**, 1935